



HAL
open science

Long-lasting and controlled antioxidant property of immobilized gold nanoparticles for intelligent packaging

J. Beurton, I. Clarot, J. Stein, B. Creusot, C. Marcic, E. Marchioni, A. Boudier

► To cite this version:

J. Beurton, I. Clarot, J. Stein, B. Creusot, C. Marcic, et al.. Long-lasting and controlled antioxidant property of immobilized gold nanoparticles for intelligent packaging. *Colloids and Surfaces B: Biointerfaces*, 2019, 176, pp.439-448. 10.1016/j.colsurfb.2019.01.030 . hal-02018092

HAL Id: hal-02018092

<https://hal.univ-lorraine.fr/hal-02018092>

Submitted on 21 Oct 2021

HAL is a multi-disciplinary open access archive for the deposit and dissemination of scientific research documents, whether they are published or not. The documents may come from teaching and research institutions in France or abroad, or from public or private research centers.

L'archive ouverte pluridisciplinaire **HAL**, est destinée au dépôt et à la diffusion de documents scientifiques de niveau recherche, publiés ou non, émanant des établissements d'enseignement et de recherche français ou étrangers, des laboratoires publics ou privés.



Distributed under a Creative Commons Attribution - NonCommercial 4.0 International License

Long-lasting and controlled antioxidant property of immobilized gold nanoparticles for intelligent packaging

J. Beurton¹, I. Clarot¹, J. Stein¹, B. Creusot¹, C. Marcic², E. Marchioni², A. Boudier^{1*}

¹ Université de Lorraine, CITHEFOR, F-54000 Nancy, France

² Université de Strasbourg, CNRS, IPHC UMR 7178, F-67000 Strasbourg, France

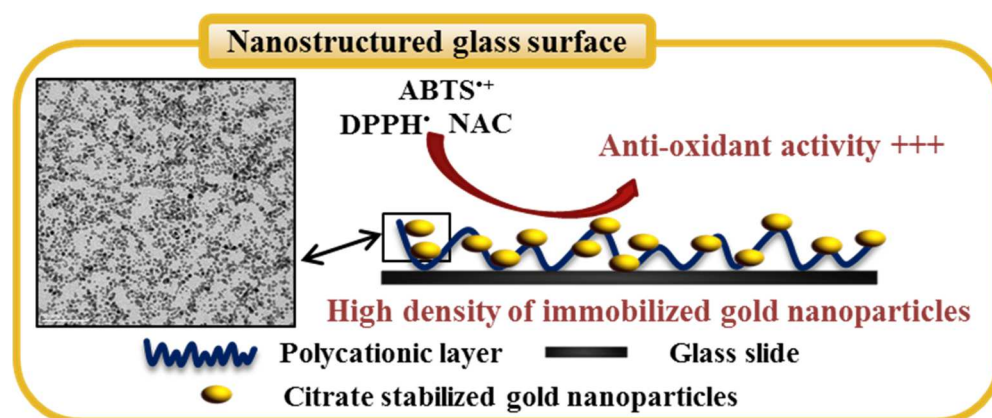
* Corresponding author.

Phone +33 372 747 228

ariane.boudier@univ-lorraine.fr

Highlights

- Nanostructured surfaces made of immobilized gold nanoparticles
- Short and long-lasting anti-oxidant capacity against free-radical species
- Enhancement of reduced thiol half-life
- High density of immobilized gold nanoparticles may form an intelligent packaging



Abstract

The development of new packaging able to preserve sensitive biomolecules against oxidative stress is an important field. Several studies refer to antioxidant properties carried out by colloidal gold nanoparticles (AuNP). Herein, the purpose was to check whether this property is preserved when AuNP are immobilized on a glass support. After nanostructured film preparation, the physicochemical characterization proved that AuNP were well-individualized in the films with a high density of immobilization. Two radicals: ABTS^{•+} and DPPH[•] were used to investigate their antioxidant capacity. The results showed that immobilized AuNP had a preserved antioxidant capacity characterized by a different kinetic: more controlled and more prolonged but with the same efficiency (vs the same quantity of colloidal AuNP). The AuNP films demonstrated a capacity to prevent from degradation a molecule containing a thiol function. A 10-fold increase of N-acetylcysteine half-life was measured using the immobilized AuNP, highlighting the interest of the developed and adaptable support.

Keywords: AuNP, nanostructured films, physicochemical characterization, antioxidant, radicals, storage

1. Introduction

Gold nanoparticles (AuNP) are nowadays part of the most developed and used nanomaterials because of their ease of synthesis and their characteristics which implies their numerous applications and their biocompatibility [1–3]. They are well defined by their physicochemical and optical properties which result from their structure. AuNP can be functionalized by biomolecules and drugs with important yield due to an important surface over volume ratio [2,4]. Numerous studies are describing the antioxidant properties of AuNP [5–7]. The particles can directly scavenge free radical species *via* catalytic reaction on their surface after adsorption of the molecule. This allows an interaction between the unpaired electron from the free radical and the conduction-band electron of the AuNP providing an enhanced antioxidant property [5]. They can also act as antioxidant delivery systems after drug grafting on their surface [7]. Gold nanoparticles were shown to increase the antioxidant potency of molecules such as Trolox®, the hydrophilic derivative of vitamin E [6], ascorbic acid [5] or reduced glutathione [4].

In parallel, food or cosmetic storage in daily life is an important domain of nanotechnology application through packaging and the related business is continually increasing [3,8].

Packaging is qualified by Samuelsson (2017) as:

- active: when it creates an inert barrier between food and the environment and reacts with the food product for extension of its preservation,
- intelligent or responsive: when it can detect, sense, record, trace, communicate, and apply a scientific interpretation to increase shelf life, enhance safety, improve quality, provide information, and warn about possible problems.

Oxidative stress is a main parameter to control in order to ensure a good storage of food and cosmetics. This may lead to a loss of nutrients, or the degradation of the interesting molecules in the case of cosmetics (antioxidant, lipids, ...), and to a generation of undesirable flavors or even potentially toxic substances [9,10]. To replace phenolic antioxidant components that are questioned towards their potential toxicity such as for example butylated hydroxyanisole (BHA) and butylated hydroxytoluene (BHT), other strategies must be developed [11]. In this way, some nanotechnologies are nowadays under investigation to be used in food processing and/or packaging to prevent oxidation of sensitive goods [3]. This intelligent packaging usually includes a matrix, based on cellulose or gelatin, combined with nanomaterials [11–13]. Despite their interesting antioxidant property, AuNP are poorly studied in this application. AuNP can be functionalized by several kinds of small molecules, polymers or

even protein and antibodies [14–18] which can also facilitate their anchorage on the support [14,17]:[19]. However, few reports described the immobilization of AuNP on matrices to develop new packaging and authors only studied the antioxidant property of the material in a short-term issue [20,21].

In this work, a polymer film immobilizing a high density of AuNP was created and characterized. Its antioxidant property was studied according to short-term and long-term endpoints monitoring the kinetic in comparison to colloidal AuNP. The preservation of a molecule containing a thiol function was also tested as a proof of concept.

2. Materials and Methods

2.1. Reagents and standards

All reagents and solvents were of analytic grade and used without further purification. KCl was purchased from Carl Roth. Citric acid and KH_2PO_4 were purchased from Labosi. Methanol and Na_2HPO_4 were purchased from Carlo Erba. $\text{K}_2\text{S}_2\text{O}_8$, NaOH 30%, NaCl and HCl 1 M were purchased from VWR Chemicals. Phosphate buffer saline solution (PBS) was prepared as follows: $[\text{Na}_2\text{HPO}_4] = 6.68 \times 10^{-3}$ M, $[\text{KH}_2\text{PO}_4] = 1.47 \times 10^{-3}$ M, $[\text{NaCl}] = 138.00 \times 10^{-3}$ M, and $[\text{KCl}] = 2.68 \times 10^{-3}$ M, final pH was adjusted to 7.4. Tris-HCl buffer was obtained by dissolving 18.16 g of Tris in 1 L of H_2O , pH was adjusted to pH = 7.4 with HCl 12 M. All other reagents were supplied by Sigma Aldrich. Ultrapure deionized water (> 18.2 M Ω cm) was used for the preparation of all solutions.

Poly(allylamine hydrochloride) powder (PAH) and branched poly(ethylene imine) (PEI) solution 50 % wt in water with average molecular masses of 17,500 and 80,000 respectively were purchased from Sigma Aldrich.

2.2. Synthesis of citrate-stabilized AuNP

Citrate stabilized AuNP were synthesized in aqueous solution according to our previous work [22]. Briefly, 1 mL of HAuCl_4 solution (10 mg/mL) was added into 90 mL of water and 2 mL of sodium citrate 55 mM was added under inert atmosphere. The solution was stirred for 1 min then 1 mL of NaBH_4 19.5 mM was added and the solution was stirred for 10 min under nitrogen. The pH of the resulting solution was 5.5. This synthesis provides a reaction yield of 99.6 ± 0.4 % [23]. Characteristics of the resulting colloidal gold nanoparticles were demonstrated reproducible and with a low polydispersity by our previous works [24]. The synthesis was stored in the dark at 4°C during a maximum period of 20 days [24]. All experiments involving colloidal gold nanoparticles were carried out with this synthesis product without any further treatment.

2.3. Preparation of AuNP films

Borosilicate glass slides (24 x 36 mm) from Menzel-Gläser were immersed for 15 min and at 100°C in a solution of 0.1 M sodium dodecyl sulfate and then rinsed with distilled water before being immersed for 15 min and at 100°C in 0.1 M HCl solution and again rinsed with distilled water. Slides were then dried on an absorbent paper.

Polyallylamine hydrochloride and polyethyleneimine solutions were prepared at 0.1M of polymer in 10 mL of Tris-HCl buffer. The films were then made by soaking the slides in 10

ml of 0.1 M polyallylamine hydrochloride or polyethyleneimine solutions in Tris-HCl solution (10 min) and then in 10 ml of 0.15 M Tris-HCl buffer (3 min). Slides were then deposited successively in a bath of AuNP for 10 min and then in a bath of Tris-HCl buffer for 3 min. This cycle was repeated 15 times. The AuNP solutions were renewed every 5 deposits. For Transmission Electron Microscopy (TEM), the films were deposited on carbon covered copper grids (Agar) using the previous protocol but decreasing the incubation time from 10 and 3 min to 3 and 1 min respectively. A washing of 1 min in water was added after the last bath of Tris-HCl buffer.

2.4. Gold quantification using an ion pairing HPLC-vis method

The dosage of the gold was performed according to the method developed by the laboratory [23,25]. Briefly, the gold nanoparticles were first oxidized (with the solution of HCl-NaCl-Br₂) to allow the formation of an ion pair between tetrachloroaurate anion and Rhodamine B. Previous work proved that the oxidation of AuNP (Au(0)) was a total reaction and led to Au(III) ions[23]. This ion pair obtained was then extracted using an organic solvent and the corresponding Rhodamine B was quantified by HPLC/UV. In this study, glasses were crushed, rinsed in 1.0 mL of HCl-NaCl-Br₂ solution (1.000 M – 0.300 M – 0.025 M respectively), and stirred during 20 min (600 rpm). HPLC was carried out on a SpectraSystem system constituted by the following modules: vacuum degasser (SCM1000), quaternary pump (P1000XP), autosampler (AS300) and UV-visible detector (UV2000). The column (Nucleosil® C18, 150 mm × 4.6 mm, 3 μm particles size and 100 Å porosity) was thermostated at 40 °C using a Croco-cil (1267) oven. Data acquisition and injection control were performed by the Azur software (version 5.0, Datalys®). The isocratic mobile phase consisted on a binary mixture of acetonitrile and 0.1 % trifluoroacetic acid aqueous solution (25/75, V/V). The injection volume was 20 μL. The detector was set at a wavelength of 555 nm and the pump at a flow rate of 1.0 mL min⁻¹.

2.5. Reduction of 2,2'-azino-di(3-ethylbenzothiazolin-6-sulfinate) by immobilized AuNP

An 2,2'-azino-di(3-ethylbenzothiazolin-6-sulfinate) (ABTS^{•+}) stock solution was prepared by dissolving 20 mg of ABTS in 6 mL of PBS and mixing this solution with 1 mL of 1.3 mM K₂S₂O₈ with an overnight incubation. An appropriate dilution of the solution (final concentration 6.7 mM) was operated just before its use ($\epsilon_{734\text{nm}} = 1.5 \times 10^4 \text{ M}^{-1} \text{ cm}^{-1}$) [22]. Antioxidant capacity of colloid and immobilized gold nanoparticles were compared by using ABTS^{•+}. For this purpose, the volume of colloidal AuNP containing the same number of

nanoparticles to the one present on a slide was calculated. Glass Surface covered by the film is 8.64 cm². Quantification of gold nanoparticles on that part of the slide led to an immobilization density of 3.8 x 10¹³ AuNP/cm². So, one slide contains 3.2 x 10¹⁴ AuNP. Considering the Avogadro's number (6.022 x 10²³), this value corresponded to 5.3 x 10⁻¹⁰ moles of nanoparticles. According to a concentration of 69.3 x 10⁻⁹ M of colloidal AuNP at the end of the synthesis, the corresponding volume was 7900 μL. This calculation allowed the comparison of immobilized *vs* colloidal nanoparticles. The kinetic (t = 0, 0.25, 0.5, 1, 2.5, 4, 5 and 6 h) of variation of ABTS^{•+} absorbance at 734 nm were studied in triplicate. The samples were placed in a water bath, in the dark, at a temperature of 37°C and a stirring of 50 rotations per min. In parallel, controls at the same dilution of ABTS^{•+} were realized as follow: with GSH (as a reference antioxidant positive control (*ca.* 5 mg,)) or with slides covered with only PAH film or uncovered slides. The negative control was realized with only ABTS^{•+} solution incubated in similar conditions.

To study the long-lasting reducing capacity of immobilized gold nanoparticles, the following protocol was performed. Several ABTS^{•+} reduction cycles (cycle of 6h) were repeated (12 times) on the same slides covered with 15 deposits according to the previous cited conditions. The slides were placed for several cycles of 6 hours under the same conditions with a fresh solution of ABTS^{•+} prepared as described above. The experiments were carried out in triplicate. Absorbances were measured at λ = 734 nm at t = 0 min and at t = 6 h for each cycle. The difference in ABTS^{•+} concentration between negative controls and samples at the end of the 6 h cycle was calculated as:

$$\% \text{ Difference} = \frac{([ABTS^{•+} \text{ control}] - [ABTS^{•+} \text{ slide}])}{[ABTS^{•+} \text{ control}]} \times 100$$

Where [ABTS^{•+}control] is the concentration of ABTS^{•+} in negative controls and [ABTS^{•+}slide] is the concentration of ABTS^{•+} in samples with slides after 6 h.

2.6. Reduction of 1,1-diphenyl-2-picryl-hydrazyl by immobilized AuNP

The stock solutions of DPPH[•] and its reduced form DPPH₂ were prepared by dissolving 28 mg of DPPH[•] and DPPH₂ in 100 mL of methanol (71 μM). The working solutions were obtained by diluting the stock solutions by 10-fold in a methanol-10 mM citrate ammonium buffer pH 7.4 (60/40, V/V) according to [26] (this medium did not alter the AuNP film). To monitor at the same time both DPPH[•] and DPPH₂ concentrations, a separative method was used [26]. HPLC was carried out with similar chromatographic materials than in 2.4 except

the isocratic mobile phase which consisted on a mixture of methanol and 10 mM citrate ammonium buffer pH = 7.4 (80/20, V/V). The column was thermostated at 40 °C using a Croco-cil oven and the injection volume was 100 µL. The detector was set at a wavelength 330 nm and the pump at a flow rate of 1.0 mL.min⁻¹. Data acquisition and injection control were performed by the Azur software (version 5.0, Datalys®).

The reduction of DPPH[•] into DPPH₂ by immobilized AuNP was studied in triplicate. The samples were placed in the dark and in a water bath at a temperature of 37°C and a stirring of 50 rotations per min. Chromatography analyses were performed at t = 0, 0.25, 0.5, 1, 2, 4 and 5 h. In parallel, controls at the same dilution of DPPH[•] were realized as follow: with GSH (as a reference antioxidant positive control (*ca.* 5 mg,)) or with slides covered with only PAH film or uncovered slides. The negative control was realized with only DPPH[•] solution incubated in similar conditions.

2.7. *N*-acetylcysteine quantification

A 6.7 µM solution of *N*-acetylcysteine was prepared in Phosphate Buffered Saline (0.148 M; pH = 7.4). The ability to maintain *N*-acetylcysteine under its reduced state by immobilized AuNP was studied by soaking glass slides covered by AuNP films in 15 mL of *N*-acetylcysteine solution during 24 h at 4 °C in the dark. The effect of AuNP quantity was also tested with films made by an increasing number (1, 3, 5, 10, and 15) of AuNP deposits. In parallel, a negative control of *N*-acetylcysteine in the same conditions was carried out. The remaining *N*-acetylcysteine concentration in the dipping solution at t = 0, 2, 4, 6 and 24 h was determined using Ellman's method. Briefly, 100 µL of 5,5'-dithio-bis(2-nitrobenzoic) acid solution (1 mM in Phosphate Buffered Saline 0.148 M; pH = 7.4) were added to 500 µL of each sample. This mixture was incubated 10 min at room temperature protected from light then absorbances were read at λ = 412 nm. *N*-acetylcysteine concentrations were calculated using a calibration curve obtained with a standard reduced glutathione solution diluted in Phosphate Buffered Saline (0.148 M; pH = 7.4) in the range of 3 to 10 µM.

A first-order rate law was considered for the calculation of the constant of kinetic using:

$$C = C_0 e^{-kt}$$

in which C is the concentration of *N*-acetylcysteine at a time t, C₀ the initial concentration and k the constant of kinetic.

The half-life was calculated using:

$$T_{1/2} = \frac{\ln(2)}{k}$$

In which $T_{1/2}$ is the half-life of *N*-acetylcysteine and k the constant of kinetic.

2.8. Nanoparticle characterization

Colloidal gold nanoparticles were characterized after synthesis without any dilution step. UV–vis spectrophotometer (UV-1800 Shimadzu) was used for spectra recordings and absorbance measurements. Molar absorbance value for AuNP was $\epsilon = 1.2 \times 10^7 \text{ M}^{-1} \text{ cm}^{-1}$ [25]. The hydrodynamic diameter (D_h) and zeta potential (ζ) of AuNP were measured at $20 \pm 1^\circ\text{C}$ using a Zetasizer Nano ZS (Malvern Instruments, UK). Transmission Electron Microscopy (TEM) images were recorded using a Philips CM20 instrument with a LaB_6 cathode at 200 kV. DigitalMicrograph software was used to determine AuNP core diameters by measuring 200 individualized nanoparticles. Energy dispersive X-ray spectroscopy (EDS) was performed on a part of a grid.

3. Results and Discussion

3.1. Colloidal AuNP

Gold nanoparticles were synthesized according to a previously validated protocol [24]. Their physicochemical characterization was performed and results are presented in Figure 1. The spectroscopic properties of the particles showed a Localized Surface Plasmon Resonance (λ_{max}) at 514 nm without any other peak meaning no aggregation [27]. This parameter is specific to metallic nanoparticles and gives information on their size, their form, their environment in terms of medium, and neighbor particularly the inter-nanoparticulate distance [28]. Hydrodynamic and core diameters were respectively 6.5 and 2.7 nm. The difference between those 2 dimensions represents the stabilization and the solvation layers. The charge surface was negative which was explained by the presence of citrate ions used as capping agents of AuNP. The assay and concentration were conform to our previously published results [22,25,29].

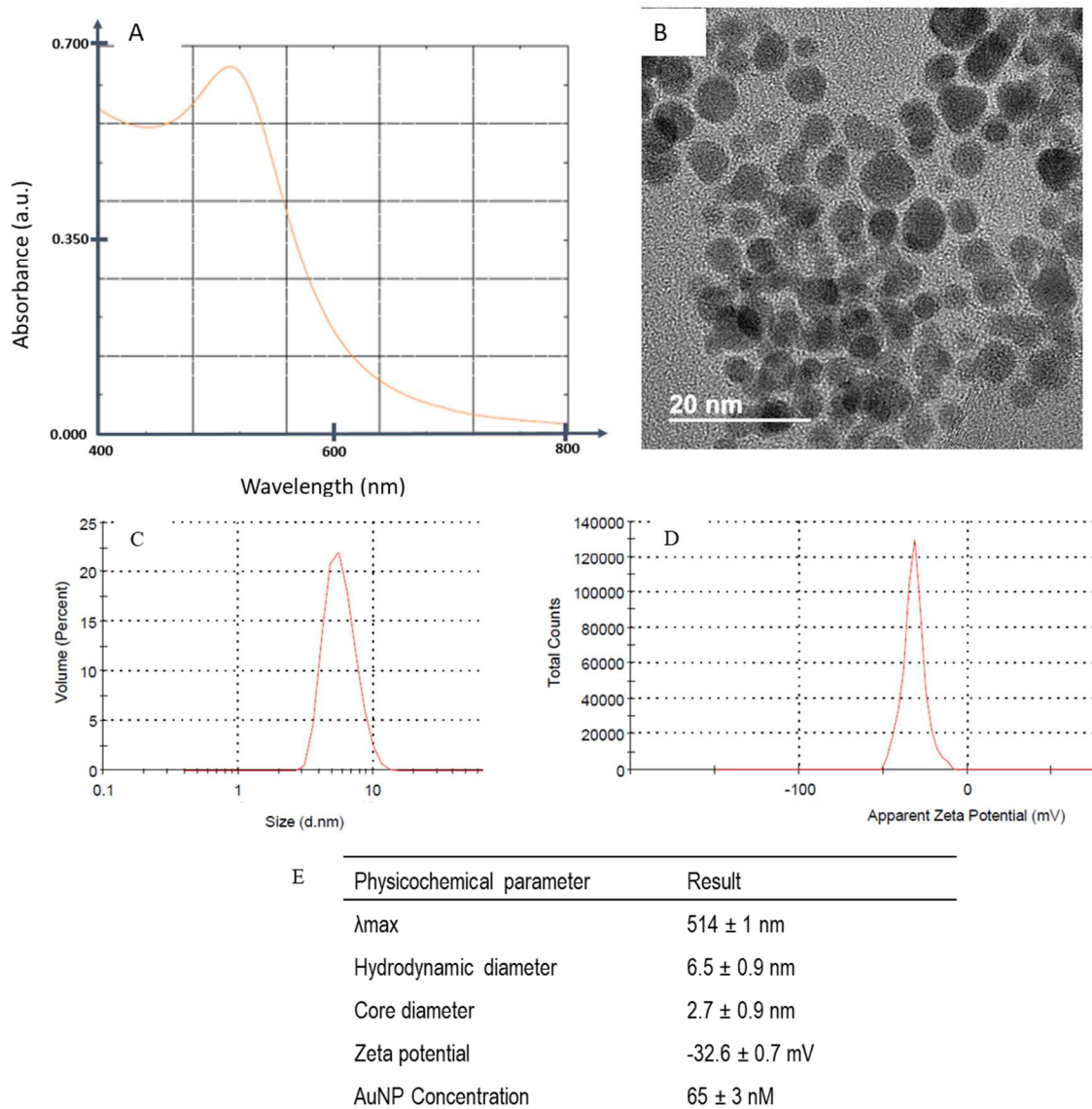


Figure 1. Physicochemical characterization of colloidal AuNP using (A) spectrophotometry, (B) TEM, (C) Dynamic Light Scattering, (D) Laser Doppler Electrophoresis and the whole results (E).

3.2. Characterization of films containing immobilized AuNP

Films immobilizing AuNP were prepared by soaking baths through electrostatic interactions [30]. After glass cleaning, and thanks to the negatively charges (silanol groups) present on the glass surface, a monolayer of a polycation (polyallylamine, ionization constant, $pK_a = 8.7$ [31]) was first deposited to create a positively charged surface in order to successively anchor the negatively charged particles, up to 15 deposits.

The created films were fully characterized using spectrophotometry, TEM equipped with EDS and a method to quantify gold. The corresponding results are shown in Figure 2 and 3. The

spectroscopic results highlighted the presence of the Localized Surface Plasmon Resonance confirming the signature of AuNP which were observed in TEM (Figure 2A and 3A). EDS study was performed on a part of a TEM grid and the corresponding elemental analysis is shown in Figure 3C. Three main elements were found: nitrogen which comes from the polymer containing a primary amine, oxygen which comes from citrate ions of AuNP capping, and gold. The value of Localized Surface Plasmon Resonance increased as the deposits (Figure 2B), proving the modification of the AuNP environment (increase in the number of neighbors and decrease of the distance between particles, as shown by TEM images) and not in size, as the particles were well-individualized (Figure 3B), nor in aggregation as seen in Figure 2B [27]. The value of Localized Surface Plasmon Resonance was almost stable after the 8th deposit demonstrating that the nanostructuration was globally homogeneous on the whole surface. The quantity of immobilized AuNP linearly increased (Figure 2C) and after the last deposit, the AuNP density was 3.8×10^{13} AuNP/cm² using an ion pairing HPLC-vis method [23]. The obtained density on a surface of 8.64 cm² corresponded to the quantity of particles contained into 8 mL of colloidal AuNP after synthesis. This highlighted the very important concentration of AuNP on the surface of the material and was in correlation with other studies [19,32]. The density of AuNP immobilization can be easily adapted as a function of the targeted application by either the number of baths of AuNP suspension or by the coated surface.

Some optimizations were performed to improve the AuNP density but did not lead to a better quantity of immobilized AuNP. Thus, the choice of polycation was tested: polyallylamine bearing one primary amine per monomer *vs* branched polyethylenimine bearing 4 primary amines, 3 secondary amines and 4 tertiary amines. At physiological pH (7.4) only two of them are ionized[33]. The number of polyallylamine layers initially deposited was increased from 1 to 3. However, neither the modification of polymer nor the increase in polycation layers initially deposited, improved the AuNP density. The standard deviation of the absorbance of those surfaces at the end of the construction was about 7 %.

The stability of the films was tested according to their spectroscopic properties. After 3 months, no significant modification was noticed in terms of absorbance (less than 0.016 a.u. of difference at the end of the study). Altogether, these results proved the nanostructuration of the support with a very important density of immobilized AuNP with good stability as a function of time.

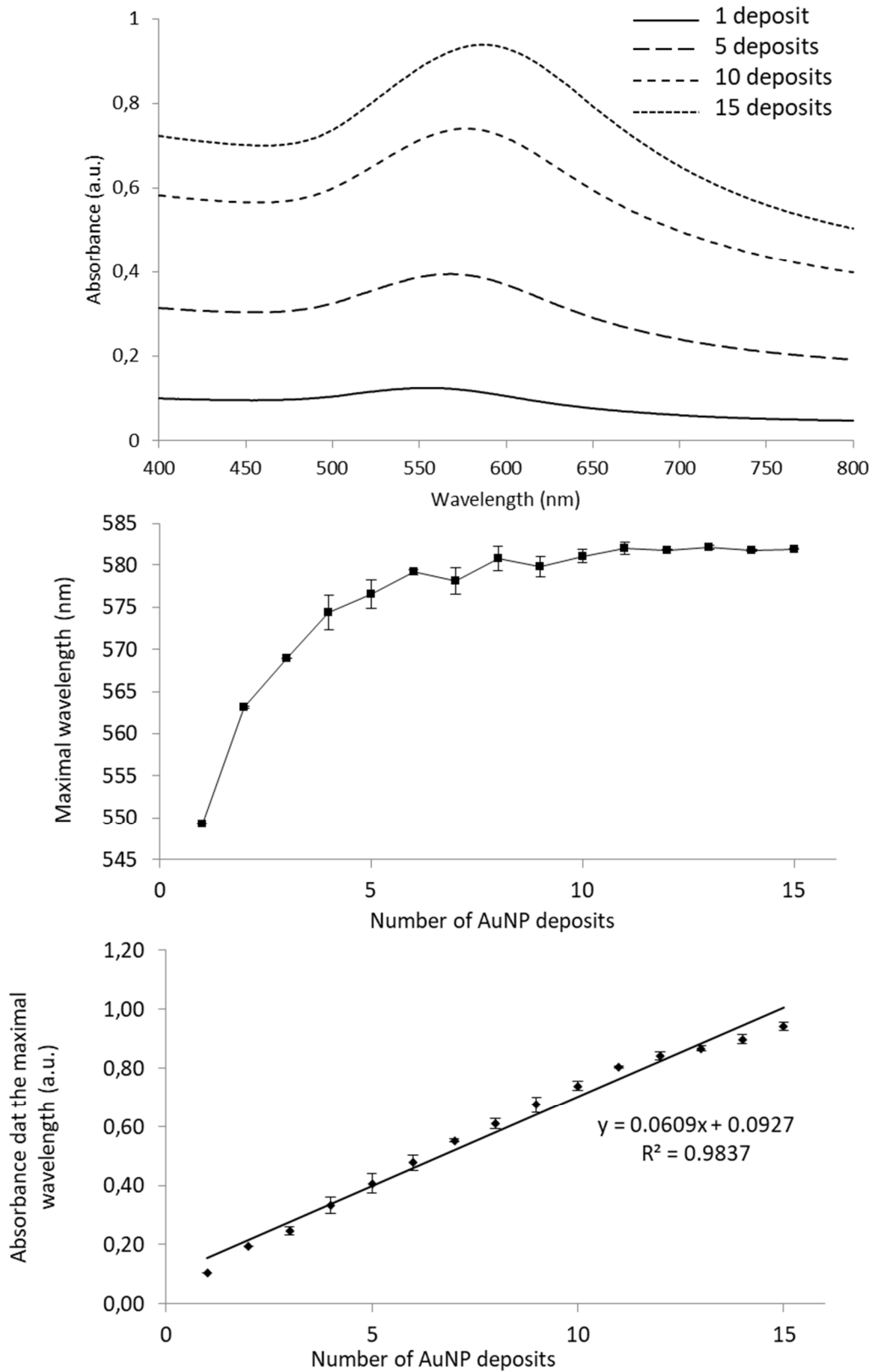


Figure 2. Spectral properties of AuNP film using spectrophotometry (A) monitoring the maximal wavelength (B) and the related absorbance (C) as a function of the number of AuNP baths ($n = 3$).

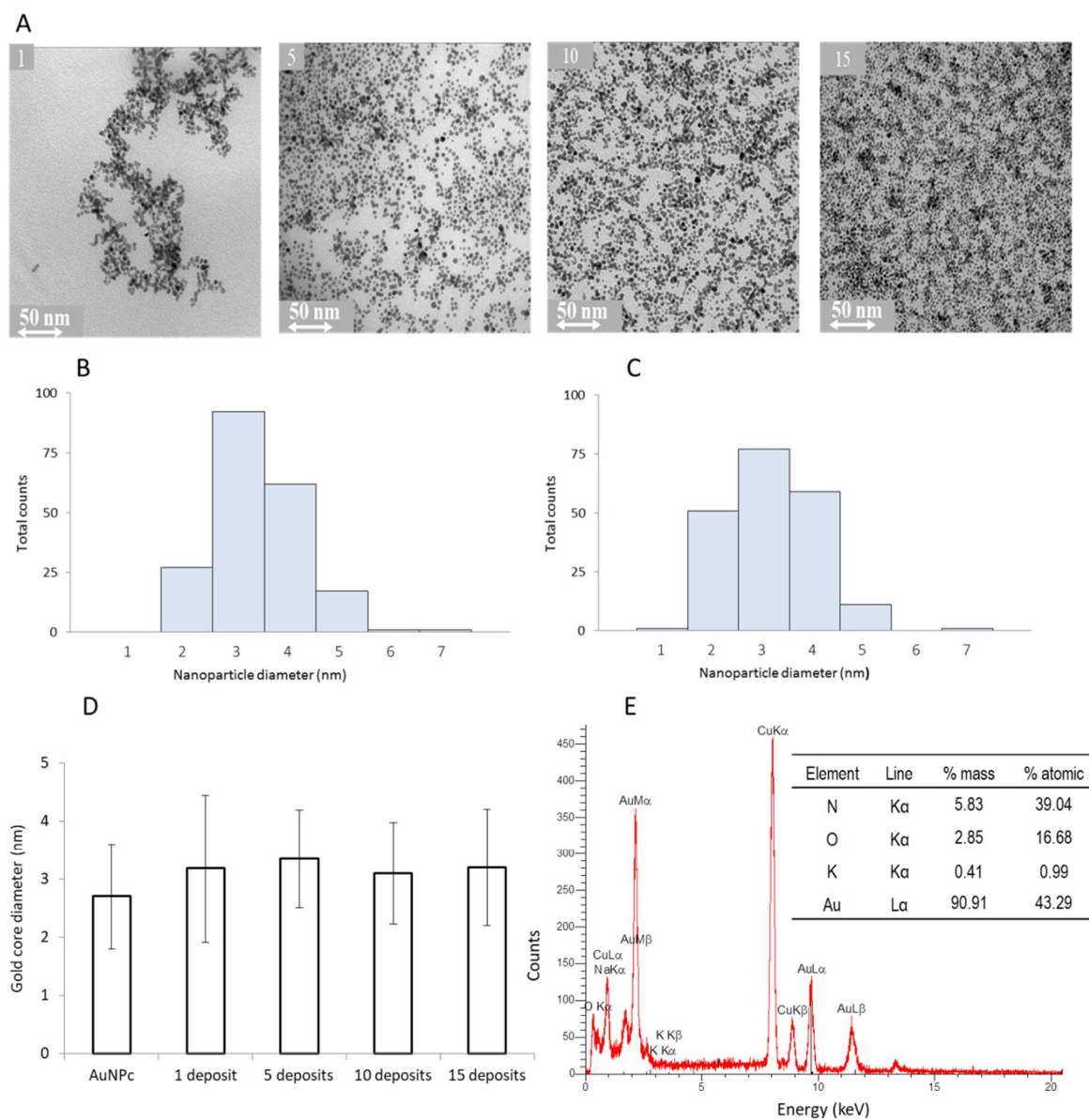


Figure 3. Characterization of films containing immobilized AuNP. Observations by TEM of films after 1, 5, 10 and 15 depositions of AuNP (A), distribution of gold core diameters ($n = 200$) for 5 (B) and 10 (C) depositions of AuNP, the mean measurement of gold core diameters (D) ($n = 200$) and EDS analysis on a film of 10 AuNP depositions (E).

3.3. Antioxidant property of the nanostructured film

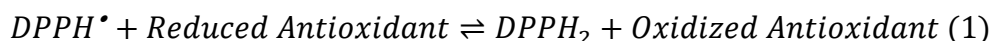
Antioxidant activity of AuNP is well-described in the literature [6,22,29,34]. However, to the best of our knowledge, the antioxidant activity of AuNP when they are immobilized on a support remains poorly studied [20,21].

The developed nanostructured material was tested using two molecules: 1,1-diphenyl-2-picryl-hydrazyl (DPPH[•]) and 2,2'-azino-di(3-ethylbenzathiazolin-6-sulfinate) (ABTS^{•+}).

These two classical antioxidant tests are based on the reduction of radical monitored by either spectrophotometry or HPLC-vis [26,35]. The performances of the support were evaluated in short-term and long-term endpoints.

3.3.1. Short-term effect

As far as the DPPH[•] test is concerned, the AuNP immobilized films showed an antioxidant property as shown by the radical reduction (Figure 4A) parallel to a production of DPPH₂, the hydrogenated product of the reaction (Figure 4B), according to equation:



This effect was only due to AuNP since glass and glass covered by the polycation did not have any effect. After 5 h of incubation, the percentages of DPPH[•] reduction by the glass (73.6 +/- 3.2 %,) and by the glass covered by polycation (77.6 +/- 0.3 %) were like the negative control (75.6 +/- 0.1 %). In parallel, the percentages of DPPH₂ production after 5 h by the glass (35.0 +/- 1.8 %), by the glass covered by polycation (32.7 +/- 0.4 %) were both similar than the negative control (30.0 +/- 0.3 %) and corresponded to the low stability of the radical in solution. The effect of immobilized AuNP was as important as the one obtained by an excess of reduced glutathione but the kinetic was more gradual using the nanostructured material. The capacity of DPPH[•] reduction by immobilized AuNP was already proven in the literature after 3 h but without any kinetic considered [21].

The ABTS^{•+} test was realized, and the results are presented in Figure 4C. The data showed the antioxidant property of immobilized AuNP. Again, this was only due to the presence of nanoparticles (the concentration of ABTS^{•+} reduction after 6 h by glass (5.0 +/- 0.1 μM), by glass covered by the polycation (4.0 +/- 0.9 μM) were in the same range than the negative control (4.9 +/- 0.1 μM)). When comparing immobilized AuNP to colloidal AuNP at the same nanoparticle quantity, two elements were interesting. First, both nanoparticle systems (immobilized and colloidal) demonstrated the same efficacy towards ABTS^{•+} reduction with a

very residual concentration (*ca* 1 μM) of the radical remaining after 6 h. Second, the kinetic of the antioxidant reaction was totally different when one compares colloidal AuNP to immobilized ones. This phenomenon was described for other AuNP contained into thin films, but the reaction was performed on model reactions (borohydride reduction of 4-nitrophenol and reaction between potassium ferricyanide and sodium thiosulfate) and not on radical species [20]. Moreover, in the cited work, the film performance was studied only up to *ca* 20 min vs 6 h, and also 3 days (*vide infra*) herein.

Our results proved that the reaction induced by immobilized AuNP was progressive and more controlled as a function of the time. Particle immobilisation induces a limitation in Brownian motion compared to colloidal AuNP which can freely move into the solution. In parallel, the polarization of the electronic cloud on the surface of the gold atoms induced by the electrostatic interaction with the polymer may lead to particles less sensitive to redox-reactions.

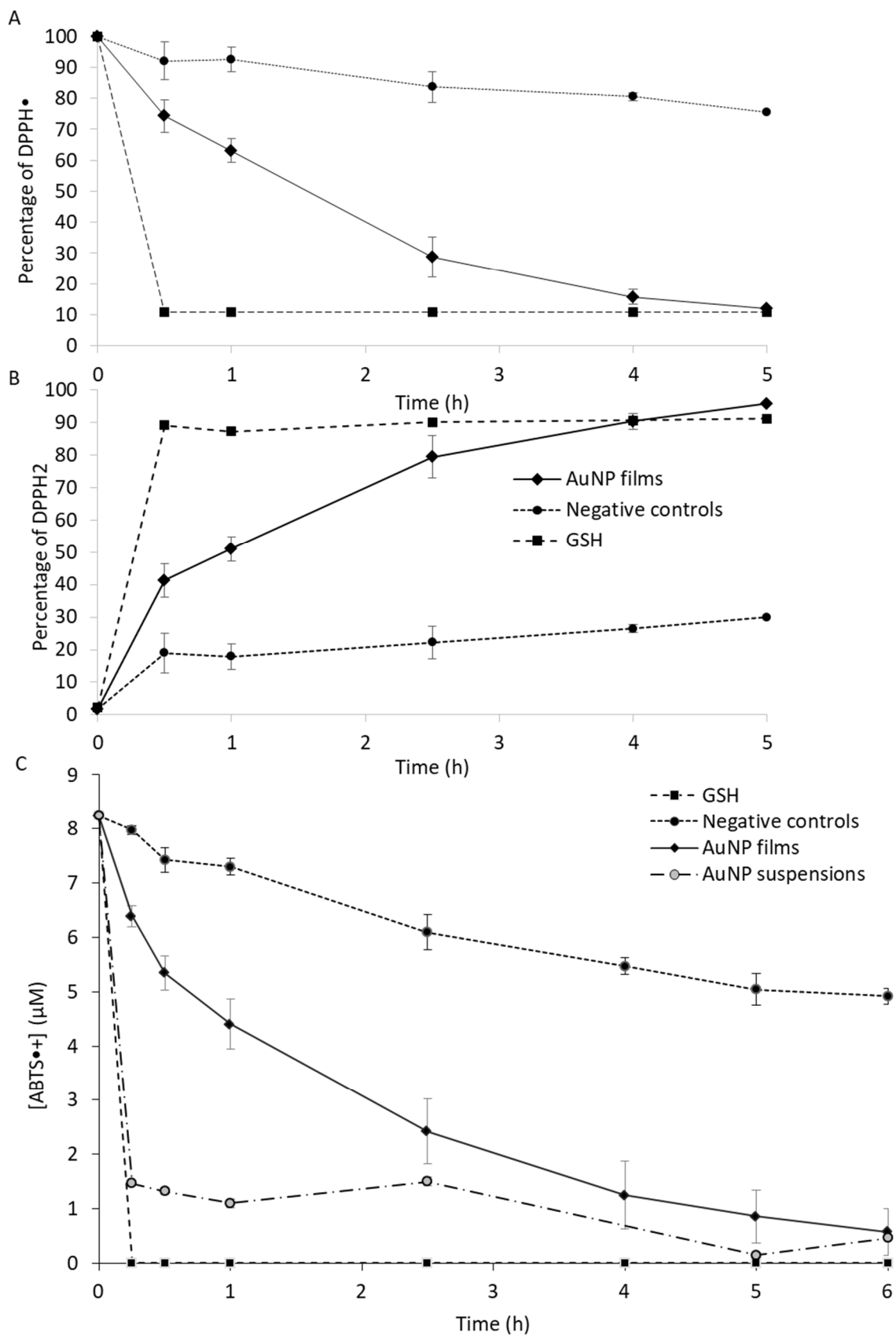


Figure 4. Antioxidant capacity of AuNP films using the DPPH•: ((A) monitoring of DPPH• disappearance and (B) DPPH₂ appearance) and ABTS•+ (C) tests (n=3).

3.3.2. Long-term effect

In a second set of experiments, ABTS^{•+} reduction by immobilized AuNP was studied with a more long-term endpoint (up to 3 days). The radical solution was replaced by a fresh one every 6 h which corresponded to the almost total reduction of the radical as previously observed in Figure 4. The long-term antioxidant effect of immobilized AuNP is illustrated by Figure 5. The obtained data showed a prolonged efficiency up to 3 days. The antioxidant effect was more important within the 12 h of experiments. Afterwards, the antioxidant property of immobilized AuNP was more progressive. The long-lasting antioxidant property of immobilized AuNP has never been described, to the best of our knowledge. However, other developed packaging proved a longer effect. A poly(lactic acid)-based nanocomposite was able to release butylhydroquinone and to have an antioxidant effect up to 6 months [11]. Gelatine films incorporated tea polyphenol nanoparticles proved the pharmacological effect up to 6 weeks [13]. In this study, the developed nanostructured materials demonstrated a shorter effect. However, our paper describes a pilot study and the materials can be adapted (coated surface, number of deposited AuNP) to reach industrial specifications for food or cosmetic matrix preservation.

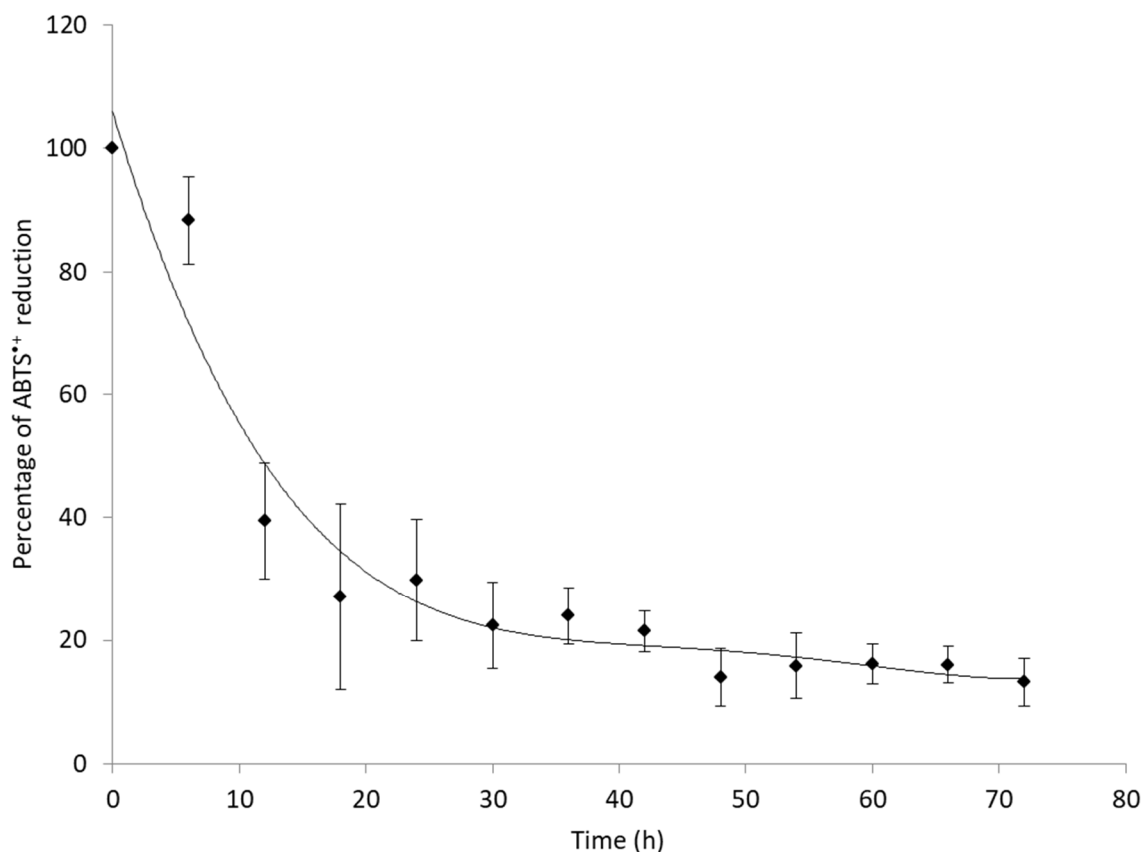


Figure 5. Long-lasting reducing capacity of immobilized AuNP by the evaluation of ABTS^{•+} reduction (the ABTS^{•+} solution was replaced by a fresh solution every 6 hours) (n = 3).

3.3.3. Effect on the storage of a molecule containing a reduced thiol function

Thiols with a cysteine residue are frequently found in food industry. For example in wine, molecules with reduced thiol function (*e.g.* glutathione, *N*-acetylcysteine) are known to preserve other aromatic thiol compounds from oxidation [36]. Improving the stability of a molecule with a thiol function under its reduced state could be a way to maintain quality of food products as a function of the time. In this way, a solution of *N*-acetylcysteine in conditions (neutral pH) that can quickly induce an oxidation was studied using a film immobilizing AuNP (Figure 6). Immobilized AuNP induced the persistence of *N*-acetylcysteine compared to the control (78.5 % vs 18.0 %, respectively). In parallel, the effect of the number of baths and consequently the quantity of immobilized AuNP was studied according to the capacity to preserve this molecule. Figure 6 shows the modelled parameters of kinetic of degradation hypothesizing a first-order rate law for this reaction. The obtained values demonstrated the more AuNP were deposited, the less important were the constant of kinetic meaning a less rapid degradation process. More interestingly, the half-life of *N*-

acetylcysteine was increased by a nearly 10-fold factor when comparing the control vs AuNP immobilized film with 15 deposits. This highlighted both the efficiency and adaptability of the system in a future application as intelligent packaging.

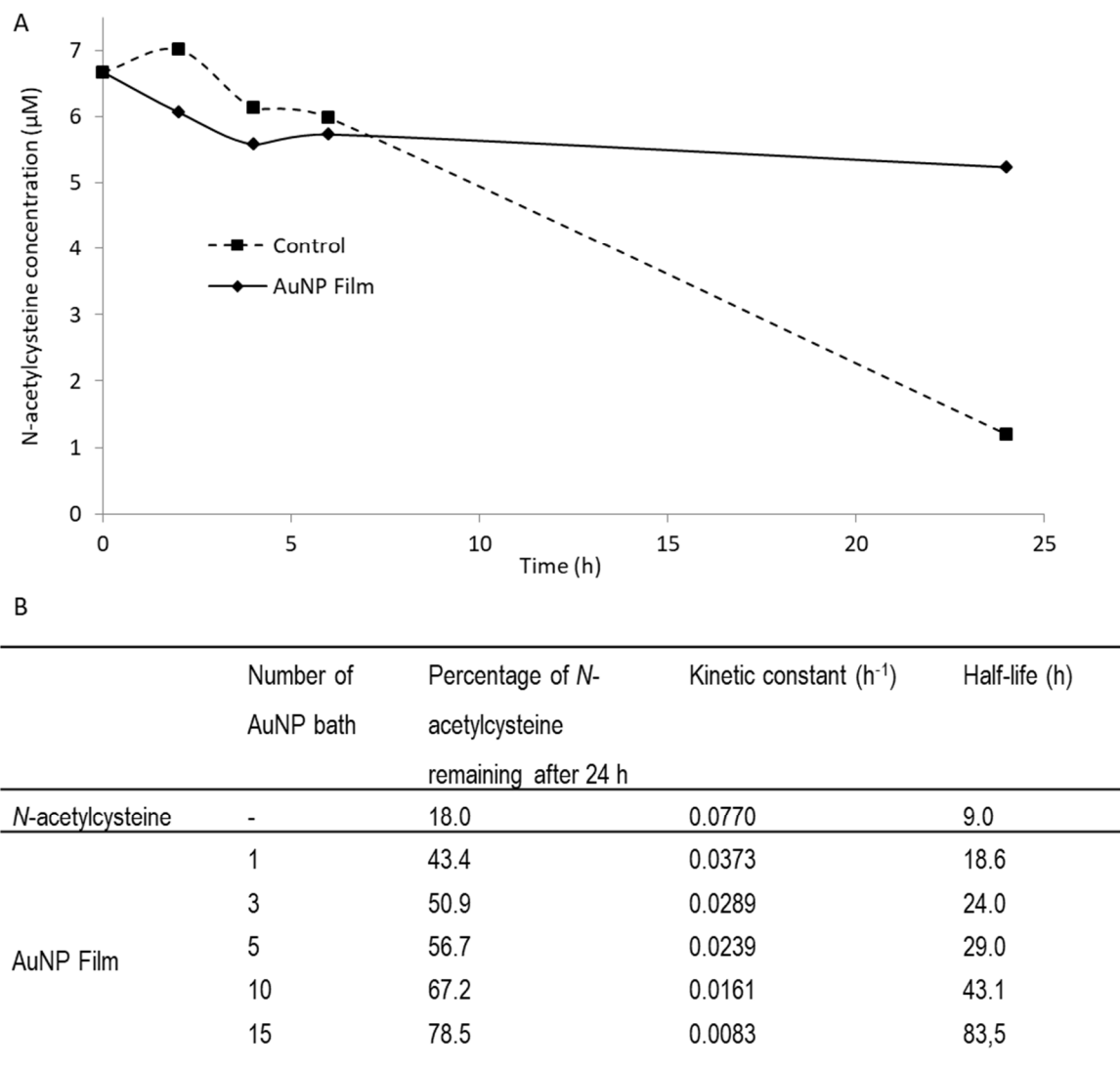


Figure 6. Antioxidant capacity of AuNP films (15 deposits) on a solution of *N*-acetylcysteine (A) and percentage of *N*-acetylcysteine and kinetic parameters of the degradation reaction as a function of the number of AuNP baths (first-order rate law at 4°C) (B).

4. Conclusion

In this paper, AuNP were immobilized on glass through electrostatic interactions. These films showed well-individualized particles with preserved spectroscopic properties. The nanostructured material revealed an antioxidant effect with a similar efficiency but different kinetic (more progressive) than colloidal AuNP. This effect was also prolonged as a function of time. Considering the adaptability of the developed prototypes (covered surface, number of AuNP deposited), the stability of the films and the long-lasting antioxidant capacity of the nanostructured material, this study laid the bases for a further development of innovative intelligent packaging to preserve biomolecules or sensitive molecules against oxidative stress in different domains such as food or cosmetics.

Declarations of interest: none

5. References

- [1] N. Elahi, M. Kamali, M.H. Baghersad, Recent biomedical applications of gold nanoparticles: A review, *Talanta*. 184 (2018) 537–556.
doi:10.1016/j.talanta.2018.02.088.
- [2] M.C. Daniel, D. Astruc, Gold nanoparticles: Assembly, supramolecular chemistry, quantum-size-related properties, and applications toward biology, catalysis, and nanotechnology, *Chem. Rev.* 104 (2004) 293–346. doi:10.1021/cr030698+.
- [3] M. Samuelsson, *Nanomaterials in Daily Life: Compounds, Synthesis, Processing and Commercialization*, Springer, 2017, Chapter 2.
- [4] M. Luo, A. Boudier, I. Clarot, P. Maincent, R. Schneider, P. Leroy, Gold Nanoparticles Grafted by Reduced Glutathione With Thiol Function Preservation, *Colloid Interface Sci. Commun.* 14 (2016) 8–12. doi:10.1016/j.colcom.2016.07.002.
- [5] H. Razzaq, F. Saira, A. Yaqub, R. Qureshi, M. Mumtaz, S. Saleemi, Interaction of gold nanoparticles with free radicals and their role in enhancing the scavenging activity of ascorbic acid, *J. Photochem. Photobiol. B-Biology.* 161 (2016) 266–272.
doi:10.1016/j.jphotobiol.2016.04.003.
- [6] Z. Nie, K.J. Liu, C.-J. Zhong, L.-F. Wang, Y. Yang, Q. Tian, Y. Liu, Enhanced radical scavenging activity by antioxidant-functionalized gold nanoparticles: A novel inspiration for development of new artificial antioxidants, *Free Radic. Biol. Med.* 43 (2007) 1243–1254. doi:10.1016/j.freeradbiomed.2007.06.011.
- [7] J. Tournebize, A. Sapin-Minet, G. Bartosz, P. Leroy, A. Boudier, Pitfalls of assays devoted to evaluation of oxidative stress induced by inorganic nanoparticles, *Talanta*. 116 (2013) 753–763. doi:10.1016/j.talanta.2013.07.077.
- [8] N. Bumbudsanpharoke, S. Ko, Nano-Food Packaging: An Overview of Market, Migration Research, and Safety Regulations, *J. Food Sci.* 80 (2015) R910–R923.
doi:10.1111/1750-3841.12861.
- [9] C.S. Yang, C.-T. Ho, J. Zhang, X. Wan, K. Zhang, J. Lim, Antioxidants: Differing Meanings in Food Science and Health Science, *J. Agric. Food Chem.* 66 (2018) 3063–3068. doi:10.1021/acs.jafc.7b05830.
- [10] M.E. Yonny, A.R. Torresi, C. Cuyamendous, G. Reversat, C. Oger, J.-M. Galano, T. Durand, C. Vigor, M.A. Nazareno, Thermal Stress in Melon Plants: Phytoprostanes and Phytofurans as Oxidative Stress Biomarkers and the Effect of Antioxidant Supplementation, *J. Agric. Food Chem.* 64 (2016) 8296–8304.
doi:10.1021/acs.jafc.6b03011.

- [11] H. Almasi, B. Ghanbarzadeh, J. Dehghannya, A.A. Entezami, A.K. Asl, Development of a novel controlled-release nanocomposite based on poly(lactic acid) to increase the oxidative stability of soybean oil, *Food Addit. Contam. Part a-Chemistry Anal. Control Expo. Risk Assess.* 31 (2014) 1586–1597. doi:10.1080/19440049.2014.935962.
- [12] P. Sonkaew, A. Sane, P. Suppakul, Antioxidant Activities of Curcumin and Ascorbyl Dipalmitate Nanoparticles and Their Activities after Incorporation into Cellulose-Based Packaging Films, *J. Agric. Food Chem.* 60 (2012) 5388–5399. doi:10.1021/jf301311g.
- [13] F. Liu, J. Antoniou, Y. Li, J. Yi, W. Yokoyama, J. Ma, F. Zhong, Preparation of Gelatin Films Incorporated with Tea Polyphenol Nanoparticles for Enhancing Controlled-Release Antioxidant Properties, *J. Agric. Food Chem.* 63 (2015) 3987–3995. doi:10.1021/acs.jafc.5b00003.
- [14] P. Samadi Pakchin, H. Ghanbari, R. Saber, Y. Omid, Electrochemical immunosensor based on chitosan-gold nanoparticle/carbon nanotube as a platform and lactate oxidase as a label for detection of CA125 oncomarker, *Biosens. Bioelectron.* 122 (2018) 68–74. doi:10.1016/j.bios.2018.09.016.
- [15] I. Venditti, T.F. Hassanein, I. Fratoddi, L. Fontana, C. Battocchio, F. Rinaldi, M. Carafa, C. Marianecci, M. Diociaiuti, E. Agostinelli, C. Cametti, M.V. Russo, Bioconjugation of gold-polymer core-shell nanoparticles with bovine serum amine oxidase for biomedical applications, *Colloids Surfaces B Biointerfaces.* 134 (2015) 314–321. doi:10.1016/j.colsurfb.2015.06.052.
- [16] E. Czechowska, K. Ranoszek-Soliwoda, E. Tomaszewska, A. Pudlarz, G. Celichowski, D. Gralak-Zwolenik, J. Szemraj, J. Grobelny, Comparison of the antioxidant activity of catalase immobilized on gold nanoparticles via specific and non-specific adsorption, *Colloids Surfaces B Biointerfaces.* 171 (2018) 707–714. doi:10.1016/j.colsurfb.2018.07.036.
- [17] S. Raeisi, A. Molaeirad, M. Sadri, H.R. Nejad, Detection of Anti-tetanus Toxoid Monoclonal Antibody by Using Modified Polycarbonate Surface, *Plasmonics.* 13 (2018) 1555–1567. doi:10.1007/s11468-017-0664-4.
- [18] I. Venditti, G. Testa, F. Sciubba, L. Carlini, F. Porcaro, C. Meneghini, S. Mobilio, C. Battocchio, I. Fratoddi, Hydrophilic Metal Nanoparticles Functionalized by 2-Diethylaminoethanethiol: A Close Look at the Metal-Ligand Interaction and Interface Chemical Structure, *J. Phys. Chem. C.* 121 (2017) 8002–8013. doi:10.1021/acs.jpcc.7b01424.

- [19] A. Pallotta, M. Parent, I. Clarot, M. Luo, V. Borr, P. Dan, V. Decot, P. Menu, R. Safar, O. Joubert, P. Leroy, A. Boudier, Blood Compatibility of Multilayered Polyelectrolyte Films Containing Immobilized Gold Nanoparticles, *Part. Part. Syst. Charact.* 34 (2017) 1600184. doi:10.1002/ppsc.201600184.
- [20] M. Biswas, E. Dinda, M.H. Rashid, T.K. Mandal, Correlation between catalytic activity and surface ligands of monolayer protected gold nanoparticles, *J. Colloid Interface Sci.* 368 (2012) 77–85. doi:10.1016/j.jcis.2011.10.078.
- [21] N. Bumbudsanpharoke, S. Ko, The green fabrication, characterization and evaluation of catalytic antioxidation of gold nanoparticle-lignocellulose composite papers for active packaging, *Int. J. Biol. Macromol.* 107 (2018) 1782–1791. doi:10.1016/j.ijbiomac.2017.10.046.
- [22] J. Tournebize, A. Boudier, O. Joubert, H. Eidi, G. Bartosz, P. Maincent, P. Leroy, A. Sapin-Minet, Impact of gold nanoparticle coating on redox homeostasis, *Int. J. Pharm.* 438 (2012) 107–116. doi:10.1016/j.ijpharm.2012.07.026.
- [23] A. Pallotta, V. Philippe, A. Boudier, P. Leroy, I. Clarot, Highly sensitive and simple liquid chromatography assay with ion-pairing extraction and visible detection for quantification of gold from nanoparticles, *Talanta.* 179 (2018) 307–311. doi:10.1016/j.talanta.2017.11.016.
- [24] A. Pallotta, A. Boudier, P. Leroy, I. Clarot, Characterization and stability of gold nanoparticles depending on their surface chemistry: Contribution of capillary zone electrophoresis to a quality control, *J. Chromatogr. A.* 1461 (2016) 179–184. doi:10.1016/j.chroma.2016.07.031.
- [25] J. Tournebize, A. Sapin-Minet, R. Schneider, A. Boudier, P. Maincent, P. Leroy, Simple spectrophotometric method for quantitative determination of gold in nanoparticles, *Talanta.* 83 (2011) 1780–1783. doi:10.1016/j.talanta.2010.12.005.
- [26] A. Boudier, J. Tournebize, G. Bartosz, S. El Hani, R. Bengueddour, A. Sapin-Minet, P. Leroy, High-performance liquid chromatographic method to evaluate the hydrogen atom transfer during reaction between 1,1-diphenyl-2-picryl-hydrazyl radical and antioxidants, *Anal. Chim. Acta.* 711 (2012) 97–106. doi:10.1016/j.aca.2011.10.063.
- [27] K. Kim, H. Ryoo, Y.M. Lee, K.S. Shin, Adsorption characteristics of Au nanoparticles onto poly(4-vinylpyridine) surface revealed by QCM, AFM, UV/vis, and Raman scattering spectroscopy, *J. Colloid Interface Sci.* 342 (2010) 479–484. doi:10.1016/j.jcis.2009.10.019.
- [28] Z.M. Qi, I. Honma, M. Ichihara, H.S. Zhou, Layer-by-layer fabrication and

- characterization of gold-nanoparticle/myoglobin nanocomposite films, *Adv. Funct. Mater.* 16 (2006) 377–386. doi:10.1002/adfm.200500450.
- [29] J. Tournebize, A. Boudier, A. Sapin-Minet, P. Maincent, P. Leroy, R. Schneider, Role of Gold Nanoparticles Capping Density on Stability and Surface Reactivity to Design Drug Delivery Platforms, *ACS Appl. Mater. Interfaces.* 4 (2012) 5790–5799. doi:10.1021/am3012752.
- [30] Z. Tang, Y. Wang, P. Podsiadlo, N.A. Kotov, Biomedical applications of layer-by-layer assembly: From biomimetics to tissue engineering, *Adv. Mater.* 18 (2006) 3203–3224. doi:10.1002/adma.200600113.
- [31] A.I. Petrov, A.A. Antipov, G.B. Sukhorukov, Base–Acid Equilibria in Polyelectrolyte Systems: From Weak Polyelectrolytes to Interpolyelectrolyte Complexes and Multilayered Polyelectrolyte Shells, *Macromolecules.* 36 (2003) 10079–10086. doi:10.1021/ma034516p.
- [32] D.M. Dotzauer, J. Dai, L. Sun, M.L. Bruening, Catalytic membranes prepared using layer-by-layer adsorption of polyelectrolyte/metal nanoparticle films in porous supports, *Nano Lett.* 6 (2006) 2268–2272. doi:10.1021/nl061700q.
- [33] R. Burgess, Use of Polyethyleneimine in Purification of Dna-Binding Proteins, *Methods Enzymol.* 208 (1991) 3–10. doi:10.1016/0076-6879(91)08003-Z.
- [34] A. Tułodziecka, A. Szydłowska-Czerniak, Development of a novel gold nanoparticle-based method to determine antioxidant capacity of Brassica oilseeds, white flakes and meal, *Food Chem.* 208 (2016) 142–149. doi:10.1016/j.foodchem.2016.03.105.
- [35] R. Van der Werf, S. Dal, J. Le Grandois, D. Aoude-Werner, F. Digel, S. Ennahar, S. Sigrist, E. Marchioni, Determination of active radical scavenging compounds in polar fruit and vegetable extracts by an on-line HPLC method, *Lwt-Food Sci. Technol.* 62 (2015) 152–159. doi:10.1016/j.lwt.2015.01.004.
- [36] I.G. Roussis, D. Papadopoulou, M. Sakarellos-Daitsiotis, Protective Effect of Thiols on Wine Aroma Volatiles, *Open Food Sci. J.* 3 (2010) 98–102. doi:10.2174/1874256400903010098.